Pergamon

PII: S0042-6989(96)00025-9

Vision Res., Vol. 36, No. 19, pp. 3183–3194, 1996

Printed in Great Britain
0042-6989/96 $15.00 + 0.00

Rod Outer Segment Renewal in the Retinae of Deep-sea Fish

ELEONORE FRÖHLICH,*† HANS-JOACHIM WAGNER*

Received 9 August 1995; in revised form 14 December 1995; in final form 10 January 1996

Outer segment renewal involves the synthesis of disc material in the photoreceptor inner segments, the shedding of the tips of the photoreceptor outer segments, and their phagocytosis by the retinal pigment epithelial cells. It has been suggested that in the retinae of deep-sea fish no renewal of outer segments may take place. In order to assess outer segment renewal in deep-sea fish retinae we counted (i) periciliary vesicles in rod inner segments as a parameter for disc-synthesis activity and (ii) phagosomes in retinal pigment epithelial cells as a parameter of shedding and phagocytosis in 12 species of deep-sea fish with multibank or single bank retinae. We also measured the lengths of rod outer segments in order to evaluate the balance between synthesis and phagocytotic activity. In four of these species (*Synaphobranchus kaupi, Nematonurus armatus, Coryphaenoides guentheri* and *Halosauropsis macrochir*) we further recorded size-related changes of these parameters and their relation to the position of a given rod within the banks in the retina. The number of periciliary vesicles was highest in inner segments of the most vitread bank and in the periphery of the retina. Phagosomes were most abundant in retinal pigment epithelial cells of the central retina. Long rod outer segments were most frequently recorded in the peripheral retina indicating that in this region new synthesis may outbalance shedding. Vitread rod outer segments were only slightly longer than sclerad ones. Larger animals had shorter rod outer segments than small ones. We present evidence that rod outer segment renewal takes place in the retina of all deep-sea fish. Vitread rods may be more active in this respect than sclerad ones. Copyright © 1996 Elsevier Science Ltd.

Retina Rods Ultrastructure Outer segment shedding Outer segment renewal

INTRODUCTION

Outer segment (OS) renewal of photoreceptors in the vertebrate retina involves two processes: the continuous synthesis of the disc-membranes and the discontinuous shedding of the tips of the OSs (Young, 1971). The tips of the OSs are ingested at the apical pole and degraded at the basal pole of the retinal pigment epithelial (RPE) cells. Disc-membranes are synthesized in the rough endoplasmic reticulum and the Golgi complex of the rod inner segment, stored near the cilium as periciliary vesicles (PCVs), transported through the ciliar bottleneck and added at the basal end of the OS (Roof, 1986).

In most deep-sea fish, photoreceptors are exclusively rods which are often arranged either in one or two layers if longer than *c.* 30 μm, or in several tiers if they are shorter than *c.* 30 μm (multibank retina) (Fröhlich *et al.*, 1995a). During lifetime, the number of banks may increase in multibank retinae (Locket, 1980). New rods are added at the retinal margin as in most other lower vertebrates (Powers & Raymond, 1990) but also inserted in more central regions into the already existing photoreceptor layer (Fröhlich *et al.*, 1995a). In multibank retinae, new rods are added from the vitread side moving older photoreceptors to the sclerad pole of the eye. In retinae with long rod outer segments (ROS) and one or two tiers of rods, ROSs are inserted at random. The differences in both the architecture of the photoreceptor layer and the proliferation pattern suggest that deep-sea fish may also differ in the mode of OS renewal.

In order to ensure a high sensitivity of rods in deep-sea fish retinae, effective absorption of photons in the OSs has to be maintained. Bleaching and photooxidation have to be counteracted by regeneration of visual pigment(s), so that a balance between renewal and removal of disc material is obtained. In spite of the low light levels in the deep-sea, calculations by Denton and Locket (1989) suggest that a significant amount of photopigment should be bleached. Furthermore, regeneration of the visual pigment in the deep-sea fish retina has been shown by Crescitelli *et al.* (1985). On the other hand, the low temperatures of the abyssal waters would contribute to minimize thermal damage of OS membranes and proteins by photooxidation and free radicals, thus reducing the

*Anatomisches Institut der Eberhard-Karls-Universität, Österbergstraße 3, D-72074, Tübingen, Germany.
†To whom all correspondence should be addressed.

need for disc renewal (Locket, 1980). The RPE in deep-sea fish retinae forms a narrow band of cells lacking the typical microvilli-like projections surrounding the OS. The volume of RPE appears to be heavily outweighed by that of the ROSs. On the basis of these observations it is conceivable that no shedding of OS tips takes place in the deep-sea fish retina.

In vivo, ROS renewal has traditionally been studied by observing the incorporation of labeled amino acids into the OS membranes (Young, 1971). Since, in most cases deep-sea fish are moribund once they come to the surface, this type of experiment cannot be carried out. Instead, approaches need to be pursued which can be performed on fixed material. We used the following parameters to monitor ROS renewal in our material: the number of PCVs indicating activity of disc-synthesis, and the number of phagosomes indicating shedding. For the evaluation of the balance between both processes the determination of ROS lengths was chosen. Although we do not know the genetically determined, species-specific ROS length, the pattern of ROS length distribution in the central and peripheral retina or in small and large specimens can be expected to indicate which of the two processes predominates. If shedding is minimal or lacking and synthesis occurs, ROS lengths will increase throughout life. If shedding occurs but no or few new discs are synthesized, ROS lengths will decrease. If shedding and synthesis are balanced, ROS lengths will be constant. In order to test these alternatives, we counted PCVs in the rod inner segments, phagosomes in the RPE, and measured ROS lengths in relation to the size of the animal and the location in the retina.

METHODS

Fish were collected during cruises 94 and 122 of RRS Challenger to the Porcupine Seabight and Goban Spur area (North-eastern Atlantic, 51 deg 20.7 min arc–49 deg 24.1 min arc N; 11 deg 24.9–15 deg 11.0 min arc W) and to Madeira (35 deg 39.30 min arc–38 deg 31.50 min arc N; 12 deg 16.08 min arc–13 deg 41.20 min arc W) and caught using a semi-balloon otter trawl (OTSB14; Merrett & Marshall, 1981) at depths ranging from about 480–4861 m. Immediately after recovery of the catch, the marine fish were identified (with the expert help of N. Merrett, The Natural History Museum, London) and their total length determined. They were prepared in the boat's own laboratory. Most of the fish were moribund, or had died during the towing of the net (13 hr). Eyes were enucleated, and eyecups or isolated retinae prepared under ambient illumination. As a rule, the left eye was processed for light microscopic immunocytochemistry, and the right eye prepared for electron microscopy. For light microscopy, tissue was fixed in 0.1 M phosphate buffer with 4% paraformaldehyde, 3% sucrose for 2–10 hr at 4°C, rinsed in buffer for 12–24 hr, transferred to 30% sucrose in 0.1 M phosphate buffer (pH 7.4) overnight and stored at −80°C. For investigations of retinal fine structure, tissue was fixed in 2.5% glutaraldehyde, 4% osmium tetroxide and stained en block with uranyl acetate. Retinae were dehydrated and embedded in Epon. Sections (1 μm) were stained with Azur II/Methylene Blue (Richardson *et al.*, 1960).

Species which were used for the determination of all parameters are listed in Table 1.

Data on PCVs and phagosomes were determined by electron microscopy. Radial sections through the retina near the exit of the optic nerve were used. Phagosomes were counted in different ultrathin sections of a given retina the total length of which added up to *ca* 700 μm. Individual counts were normalized to 1 mm. Central was defined as the inner quarter of the meridian and peripheral as the outer quarter. The remaining half was regarded as midperipheral region.

Determination of periciliary vesicles

PCVs were counted in radial ultrathin sections of rod inner segments (RISs) according to Eckmiller (1989). All vesicles located within a diameter of 2.5 μm centered around the ciliary centriole or basal body were recorded. PCVs were counted in single sections of RISs at locations where both the centriole and the cilium were seen. This criterion made sure that the maximum number of PCVs was always encountered and counts were not biased by

TABLE 1. Number of PCVs, of phagosomes and phagolysosomes and of ROS length in single, double, and multibank retinae

Species (*n* of specimens)	Range of size (cm)	Number of ROS banks	Number of PCVs per RIS section in the most proximal/most distal row	Number of phagosomes and phagolysosomes/mm RPE	ROS length (μm)
Alepocephalus agassizii (2)	21–23	1	10±5	43±8	78±18
Cataetyx laticeps (2)	21–36	1	14±6	172±25	73±7
Conocara murrayi (3)	33–35	1	12±6	87±10	58±12
Dalatias licha (1)	170	1	8±3	44	87±3
Halosauropsis macrochir (1)	44	1	11±3	30	70±7
Synaphobranchus kaupi (3)	20–24	2	10±5/8±5	100±9	66±8
Iliophys brunneus (1)	39	3	8±5/2±1	90	25±3
Antimora rostrata (3)	9–14	4	6±1/3±1	120±28	30±3
Coryphaenoides guentheri (3)	8–12	4	11±3/5±2	60±10	30±3
Lionurus carapinus (2)	31	4	22±5/10±5	66±12	32±2
Nematonurus armatus (4)	18–24	4	12±4/5±2	128±20	33±3
Trachyrhincus murrayi (1)	19	5	7±3/5±2	57	22±3

regional variations in the distribution of PCVs. This was established in preliminary experiments where a series of 20 consecutive sections through 10 RISs was evaluated. PCVs in RISs of the following retinal locations were studied: central peripheral vitread and sclerad. In each region a minimum of 30 RISs was evaluated.

For the reliable assessment of PCVs care has to be taken to investigate only samples with adequate ultrastructure. We compared the number of PCVs/section in RISs from well and poorly preserved specimens of the same species and of about the same size. The number of PCVs correlated with the state of preservation of a given retina. In poorly fixed retinae, RISs appeared "empty", membranes of the Golgi complex were not discernible and no PCVs were observed. In order to ensure an evaluation which was not influenced by artefacts, we introduced a criterion for the quality of the preservation. As the criterion structure, we chose the membranes of the Golgi complex: if these membranes were clearly seen preservation was regarded as good enough for PCV evaluation.

For the determination of a potential correlation of the number of PCVs/section and the ROS diameter, we counted PCVs in RISs sections of species with thick and thin ROSs. The following species were investigated *Aphanopus carbo*, *Gadiculus argenteus**, *Lampanyctus McDonaldi*, *Lophius piscatorius*, *Trachynotus cristulata* (mesopelagic species) and *Lionurus carapinus**, *Nematonurus armatus**, *Rouleina attrita*, *Spectrunculus grandis*, *Trachyrhincus murrayi** (bathypelagic species). Counts of PCVs in 50 RISs in the retina of one or two (*) well preserved specimen(s) per species were averaged.

Determination of phagosomes

Phagosomes and phagolysosomes were identified in ultrathin sections and counted in semithin and ultrathin sections. The nomenclature of phagosomes and their derivates was adopted from a model for OS digestion proposed by Bosch *et al.* (1993): According to this nomenclature phagosomes are ingested but not digested ROSs where discs are still discernible, whilst phagolysosomes are partly digested ROSs with the membraneous structure no longer discernible. In small retinae, the same area was evaluated by light- and by electron microscopy. In larger eyes, the region evaluated by light microscopy was divided in two to three sectors and evaluated separately by electron microscopy. In these cases the center and the far periphery of the retina were disregarded. Counts from ultrathin sections were added until approximately a total distance of 1.5–2 mm of RPE was evaluated, and the total number of phagosomes was normalized to 1 mm.

Determination of ROS length

The measurements of ROS length also include RISs because the lengths of RISs did not differ much between the species and the beginning of the RIS could be identified whereas the determination of the transition from the RIS to the ROS, in many cases, was difficult. The lengths of ROS were determined in two ways: (i) in semithin (1 μm) radial sections of Epon-embedded material (plastic sections); and (ii) in isolated ROS after dissociation of slices of paraformaldehyde-fixed retinae with papain. Retinae were incubated in 0. 1 M phosphate buffer at pH 7.4 with 1 mM L-cysteine HCl (Serva) and 20 mU/ml papain (EC 3.4.22.2 Sigma) for 2 hr at room temperature. After trituration, washing with phosphate buffer and centrifugation (12,000 rpm for 1 min) the pellet was resuspended in Kaiser's glycerol gelatin (Merck). This suspension was transferred to a slide, and RIS/ROSs were visualized with DIC optics and measured at a final magnification of ×1300 on the screen of an attached TV system. Determination in plastic sections led to an underestimation of ROSs length. Therefore, measurements of isolated ROSs were preferred.

Due to problems with tissue preservation all parameters relevant for the study of OS renewal (PCVs, phagosomes and ROSs length) could be evaluated only in 12 species (Table 1) out of a sample of more than 50 different species (Fröhlich *et al.*, 1995a,b). The retinae of most of these specimens had diameters of $\leqslant 0.5$ cm; in these cases counts of peripheral and central parts were averaged. In the case of *N. armatus*, *Coryphaenoides guentheri* (multibank retinae), *Halosauropsis macrochir* and *Synaphobranchus kaupi* (single and double bank retinae) larger retinae with adequate ultrastructure were also available. In these species, size-related changes and the impact of the eccentricity were evaluated.

RESULTS

The retinal structure of *C. guentheri* and *S. kaupi* is shown in Fig. 1(a) and (b). In *C. guentheri*, rods have short OSs which are stacked in several layers. In *S. kaupi*, rods are longer and arranged in two banks. The retinal pigment epithelium of both species is pigmented and thin. In contrast to the considerable differences in the width of the photoreceptor layer, in all deep-sea fish the inner retina is thin compared to surface-dwelling fish.

Morphology of rod inner segments and periciliary vesicles

RISs were 1.3–3.5 μm in diameter and contained large mitochondriae, rough endoplasmic reticulum, polysomes, membrane stacks of the Golgi complex and numerous PCVs (Fig. 2).

Relation of PCVs and ROSs diameter. We counted PCVs/section in species with different diameters of ROSs. From previous studies we know that, in multibank retinae, new rods are located proximal to the external limiting membrane whereas in single bank retinae older and younger rods exist side by side (Fröhlich *et al.*, 1995a). In multibank retinae, only the vitread RISs were evaluated because they represent a homogeneous population of newly formed RISs. We determined the number of PCVs in RIS sections of the midperipheral region (three locations/species) of five mesopelagic and five bathypelagic species. All ROSs with diameters $\leqslant 1.5$ μm were

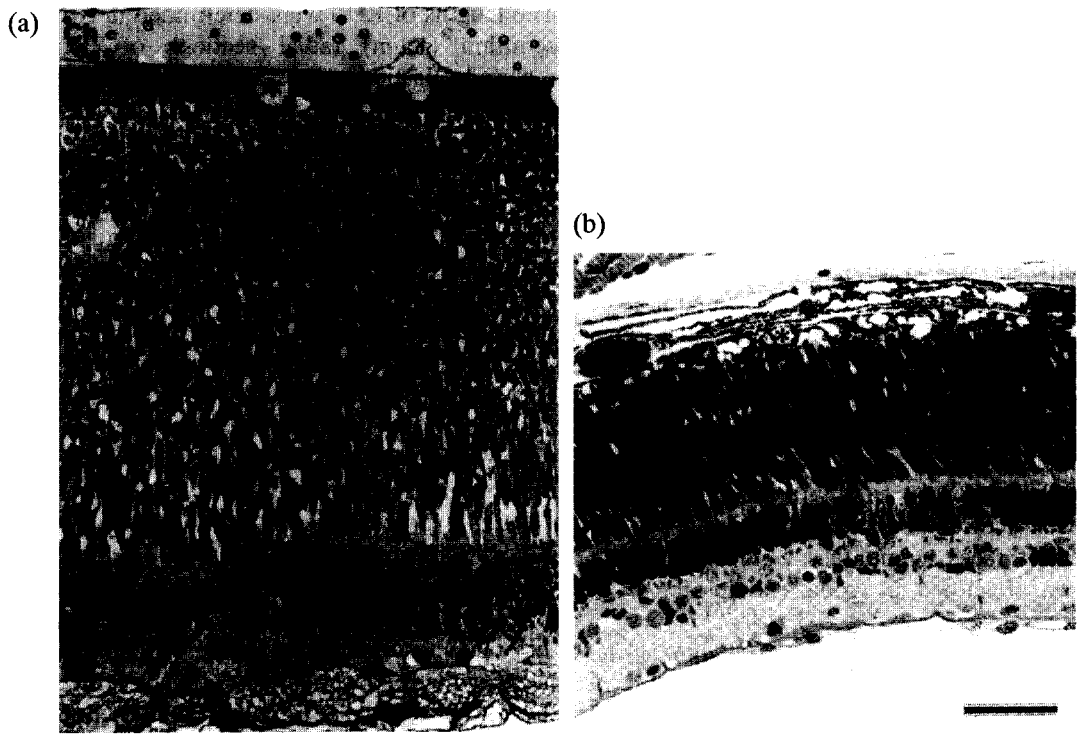

FIGURE 1. Light micrographs of 1 μm plastic sections. In *C. guentheri* (a) rods have short outer segments which are stacked in seven layers (larger specimen, midperipheral region of the eye). In *S. kaupi* (b), rods are longer and arranged in two banks (middle sized specimen, central region). In the retinal pigment epithelium of both species vesicular inclusions are seen (*). In contrast to the considerable differences in the width of the photoreceptor layer, the inner retina is thin in all deep-sea fish. Ch, Choroid; INL, inner nuclear layer; ONL, outer nuclear layer; RPE, retinal pigment epithelium; scale bar, 50 μm.

FIGURE 2. Electron micrograph of a rod inner segment of *N. armatus* with mitochondriae, polysomes, membranes of the Golgi complex and PCVs (*) surrounding the ciliary centriole (c) of the connecting cilium (cc). Scale bar, 0.5 μm.

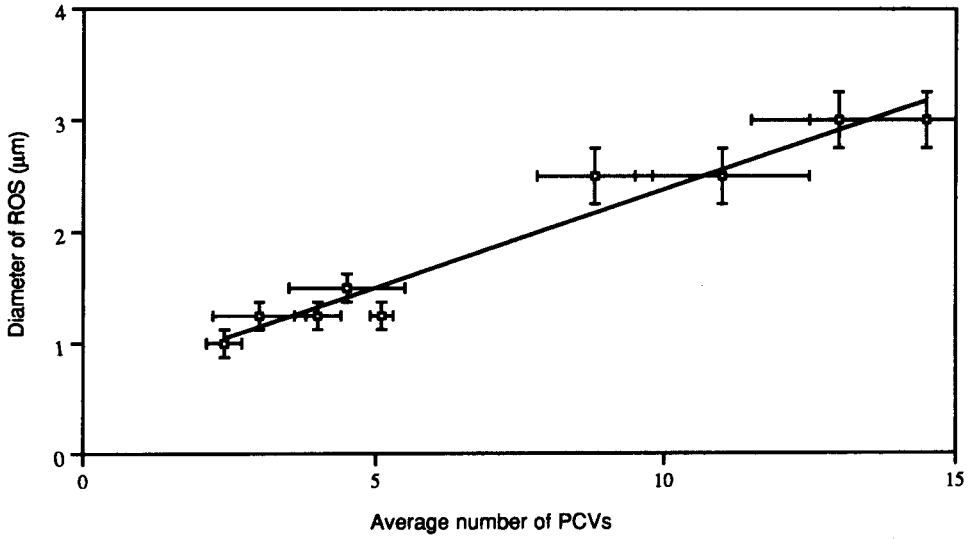

FIGURE 3. Correlation of ROS diameter and the number of PCVs per RIS section. Each point corresponds to one species.

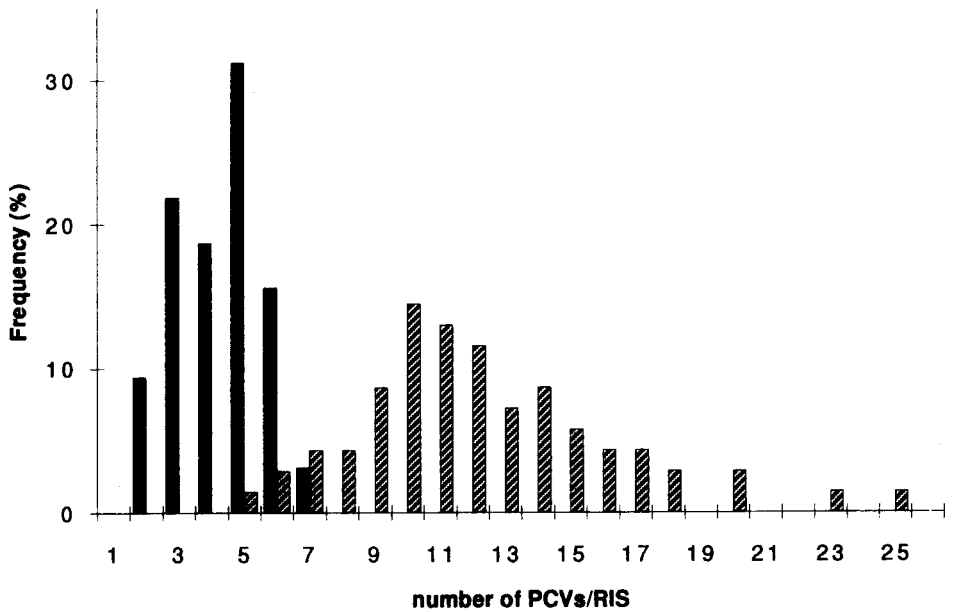

FIGURE 4. Distribution of PCVs in the multibank retina of *N. armatus*. Hatched column, vitread RISs (n = 70); solid column, sclerad RISs (n = 50).

from mesopelagic species because bathypelagic species in our samples never had ROSs with a diameter <2 µm. Figure 3 shows that there is a linear correlation between PCVs and ROS diameter. From these findings we conclude that PCV counts can be used as a reliable parameter for the activity of RISs in forming new OS membrane material in deep-sea fish.

Number of PCVs in different banks of multibank retinae. We counted PCVs in sections of sclerad and vitread RISs in multibank retinae of *N. armatus* and *C. guentheri*. In both species, PCVs/section in sclerad and in vitread RISs differ and form two separate clusters. The graph (Fig. 4) demonstrates that sclerad and vitread RISs form two different populations when based on the activity of disc-membrane formation as represented by the number of PCVs.

Number of PCVs in the central and peripheral retina. We determined the number of PCVs in sections of central and peripheral RISs in multibank retinae of *N. armatus* and *C. guentheri* and in single or double bank retinae of *H. macrochir* and *S. kaupi*. RISs in the central retina of single or double bank retinae, on average contained fewer PCVs/section than RISs in the peripheral part of the retina. The distribution pattern confirms that two populations of rods exist in the retina, one with many and another with few PCVs/section (Fig. 5). Rods with higher numbers of PCVs/section predominate in the peripheral retina, whereas rods with few PCVs/section are found more frequently in the central retina.

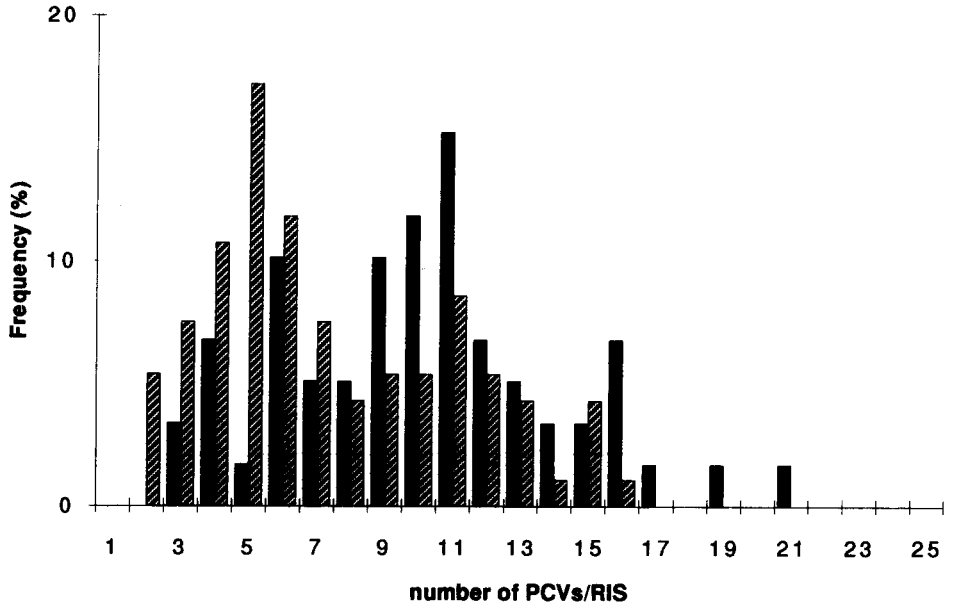

FIGURE 5. Distribution of PCVs in the single bank retina of *H. macrochir*. Hatched column, central part of the retina (n = 90); solid column, peripheral part (n = 60). Similar distribution patterns were seen in 10 specimens of four species.

Morphology of the retinal pigment epithelial cells and phagosomes

RPE cells in the present sample of deep-sea fish species were 5–20 μm high and contained variable numbers of melanosomes. Cells were attached to each other by tight junctions and desmosomes near the apical pole and showed only few and short ($\leqslant$2 μm) apical processes. The basal and the basolateral domains of the plasmalemma had smooth contours and showed occasional infoldings. Phagosomes of mostly 2–5 μm diameter near the apical pole and phagolysosomes of 1–2 μm near the basal pole were seen. The number of phagosomes was nine times higher than that of the phagolysosomes. In addition to typical phagosomes, vesicular inclusions were seen in many RPE cells (Fig. 6). These inclusions were vesicles with electron-lucent content which sometimes contained membranous residues. They were located primarily in the basal part of the RPE cells and showed great variations in diameter. Most often they were 2–5 μm in diameter; in the central part of the retina they were often larger and led to a massive vacuolization of the RPE cells (Fig. 1). The oval or sometimes lobulated nucleus was located basally in the cell. Most chromatin was present as euchromatin and often a single nucleolus was seen.

Regional differences in the number of phagosomes. The relation of phagosomes and phagolysosomes per mm did not differ between peripheral and central retina. However, the total number of phagosomes and phagolysosomes per mm was higher in the central retina (Table 2). The number and size of the vesicular inclusions increased from the periphery to the center of the retina. In larger specimens or fish with multibank retina these inclusions appeared to be more prominent.

Size-related changes of the number of phagosomes. In order to study potential size-related changes we determined the number of phagosomes/mm section in different sized individuals of the deep-sea eel *S. kaupi*. We investigated retinal radial sections passing through the exit of the optic nerve. By this standardization, we made sure that corresponding regions (peripheral and central retina) were evaluated. The number of phagosomes showed no pronounced changes from small to large specimens (Fig. 7). In small specimens, light and electron microscopic data led to similar results. In large specimens however, we found divergent results with the two techniques. Only a part of the retina investigated by light microscopy could be evaluated in the electron microscope. The region chosen for the electron microscopic evaluation was the midperipheral part. The

TABLE 2. Number of phagosomes and phagolysosomes in central and peripheral retina

Species (n of specimens)	Range of size (cm)	Phagosomes and phagolysosomes/mm RPE (central retina)	Phagosomes and phagolysosomes/mm RPE (peripheral retina)
Conocara murrayi (3)	16–33	88±20	5±2
Coryphaenoides guentheri (4)	8–19	103±32	25±8
Lionurus carapinus (3)	19–31	105±51	40±18
Nematonurus armatus (6)	18–47	139±22	34±10
Synaphobranchus kaupi (4)	18–22	100±20	22±5
Trachyrhincus murrayi (3)	19–40	130±43	10±3

FIGURE 6. Electron micrograph of retinal pigment epithelial cells in the midperipheral retina of *S. kaupi*: phagosomes (*), electron-lucent vesicular inclusions (V) and a phagolysosome (P) are seen. BM, Bruch's membrane; N, nucleus; JC, apical functional complex; ROS, rod outer segment. Scale bar, 2 μm.

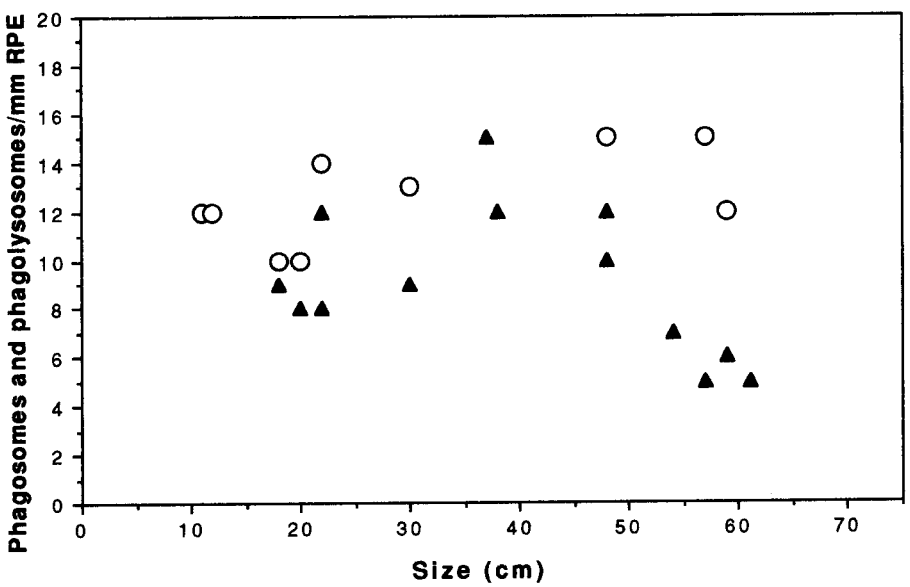

FIGURE 7. Number of phagosomes and phagolysosomes per mm section in retinal pigment epithelial cells of *S. kaupi* as a function of fish size. Light microscopic data (▲) of all retinae and electron microscopic data of small retinae are from central and peripheral sites, electron microscopic data of larger retinae are from RPE cells in midperipheral location (○).

exclusion of the central part of the retina with higher numbers of phagosomes probably led to an underestimation of phagosomes by this technique in the retinae of large specimens. There was no significant difference in the number of phagosomes/mm between multibank and single bank retinae.

In all retinae, macrophages were observed. They occurred in clusters and showed no preferential distribution with respect to a specific region of the retina. RPE cells which were surrounded by macrophages generally contained unusually high numbers of phagosomes/mm.

Morphology and length of ROSs

ROS lengths were measured in radial semithin sections and in dissociated retinae. Only measurements obtained from dissociated retinae are considered. Peripheral and central parts of the retina were evaluated separately. Broken ROS could be identified by the shape of their tips, which appeared mostly concave instead of convex or cone-like. In order to decide whether a given rod in the isolated preparation belonged to a sclerad or a vitread bank of rods (in the case of a multibank retina) we also determined the length of the myoid.

Unfortunately, however many myoids had broken off during the isolation procedure.

The shape of the ROSs differed between species but did not vary with the size of the fish in a given species. In multibank retinae, ROSs had a more cone-like appearance with a thicker proximal end and a pointed tip. By contrast, in single (or double) bank retinae ROSs were cylindrical with no pronounced variations in the diameter. The tips of these ROSs were convex (Fig. 8).

ROS length in different regions of the retina. ROS length distributions differed between the central and the peripheral part of multibank (*N. armatus*) and of double bank retinae (*S. kaupi*). In the periphery, two populations of rods were clearly distinguished whereas in the central part, this subdivision was less obvious [Fig. 9(a) and (b)]. In the retinal periphery, rods with longer ROSs predominated, whilst in the central retina most rods belonged to the population with shorter ROSs. In multibank retinae, sclerad rods could be identified by the greater length of their myoids. However, in samples of central multibank retinae, only few (10) ROSs with long myoids were observed. The average length of these ROSs was only slightly lower than the average length of all central ROSs. We therefore conclude that the pattern of ROS length distribution in sclerad rods is likely to be similar to that of vitread rods.

Size-related changes of ROS lengths. We recorded size-related changes in the retinae of *S. kaupi*, *Conocara macroptera*, *N. armatus* and *C. guentheri*. In all species ROS lengths decreased with increasing size of the animal. The decrease was linear and steeper in fish with longer ROSs (*S. kaupi*) than in those with shorter ROSs (*C. guentheri*). In the latter, ROS lengths of large individuals declined to values of about 90% of that in small ones. In large *S. kaupi* ROS were 65% of that in the small individuals (Fig. 10).

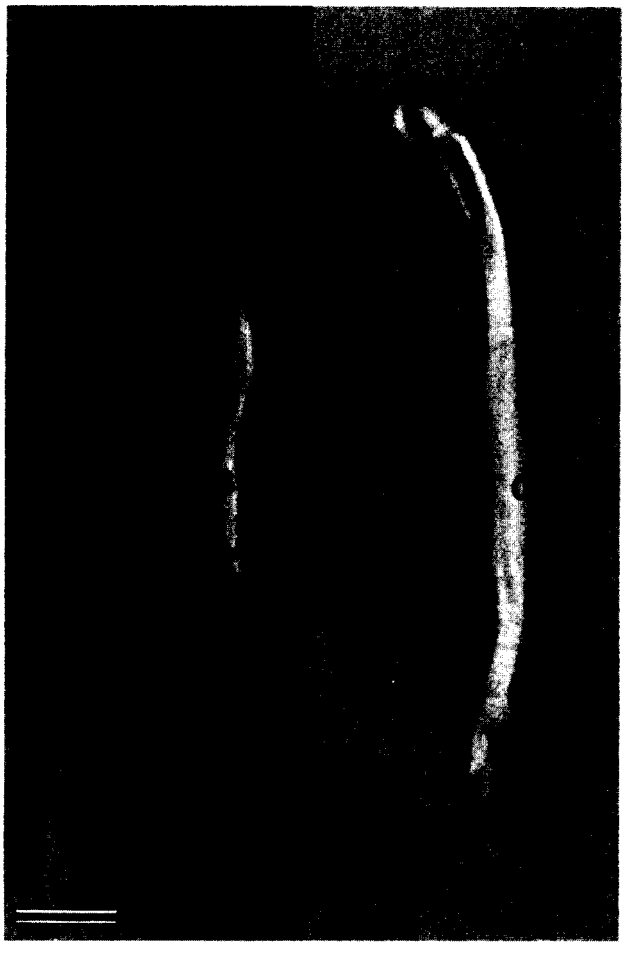

FIGURE 8. Typical shape of ROS, RIS and myoid (M) in the multibank retina of *L. carapinus* (left) and in the single bank retina of *C. macroptera* (right). In the retina of *L. carapinus* the proximal region of the ROS has a greater diameter than the distal region. The tip of the ROS is pointed. In the retina of *C. macroptera* the ROS shows no pronounced variation in the diameter from the proximal to the distal end. The tip of the ROS is convex. Scale bar, 10 μm.

DISCUSSION

We evaluated ROS renewal in the retinae of deep-sea fish by counting the number of PCVs as a parameter for new synthesis of disc material, and the number of phagosomes in the RPE cells as a parameter for shedding in the retinae of 12 different species.

Periciliary vesicles

The numbers of PCVs in RISs is determined by the balance between the activity of the Golgi complex and the speed at which they are exported through the ciliary stalk. The numbers of PCVs per RIS section differed between the central and peripheral retina, but we found no RIS in which PCVs were completely absent. This indicates that all RISs synthesize disc material, although to a different extent. As previously reported (Fröhlich *et al.*, 1995a), newly generated and differentiated rods in multibank retinae are located in the periphery and near the external limiting membrane. RISs in this region contained significantly more PCVs than centrally located and sclerad rods (Figs 4 and 11, schematics drawing).

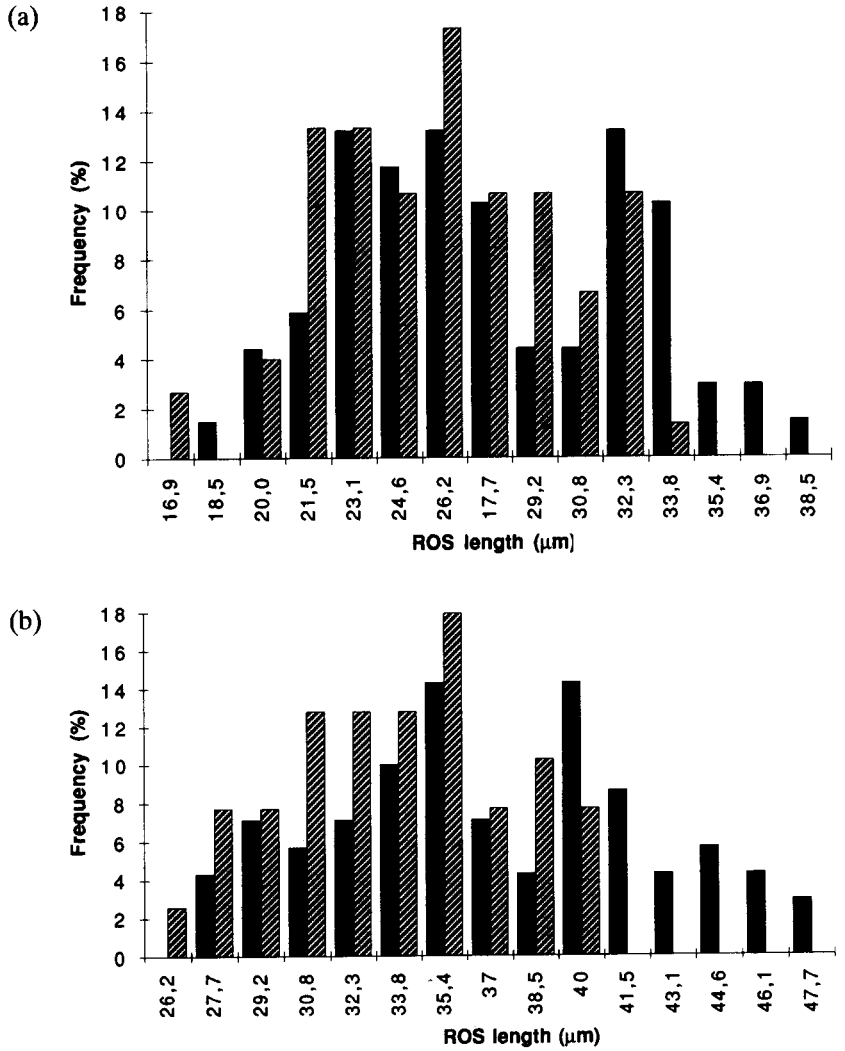

FIGURE 9. Distribution of ROS lengths in the multibank retina of (a) *N. armatus* and in the double bank retina of (b) *S. kaupi* central (hatched) and peripheral part (solid column). In total 70 central and 75 peripheral ROSs were measured for *N. armatus*, and 60 central and 75 peripheral ROS in the case of *S. kaupi*. In both types of retinae the peripheral retina contains a higher portion of long ROSs. The seemingly unequal distances of ROS length categories are the result of rounding.

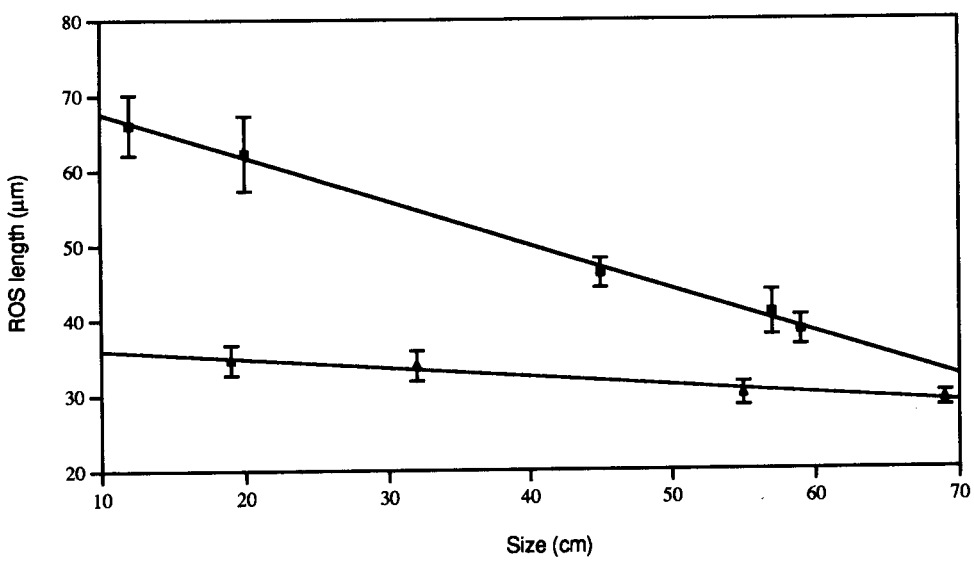

FIGURE 10. Size-related changes of ROS lengths in the double bank retina of *S. kaupi* (■) and in the multibank retina of *C. guentheri* (▲).

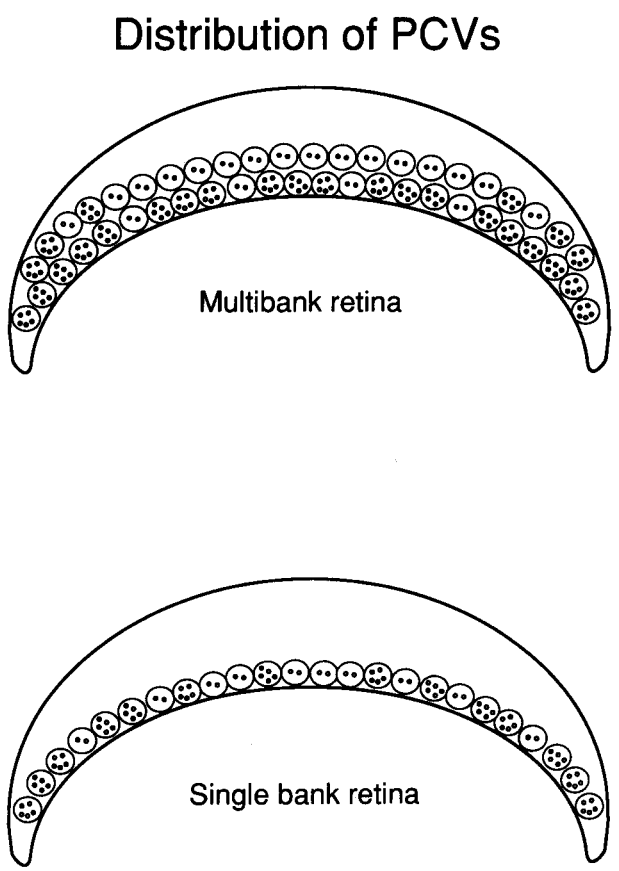

FIGURE 11. Schematic semiquantitative drawing of the distribution of PCVs in a single and a multibank retina. RISs with many PCVs predominate in the vitread bank of the multibank retina and in the peripheral part of all retinae. ⊙ represents RISs with few PCVs and ⊛ represents RISs with many PCVs.

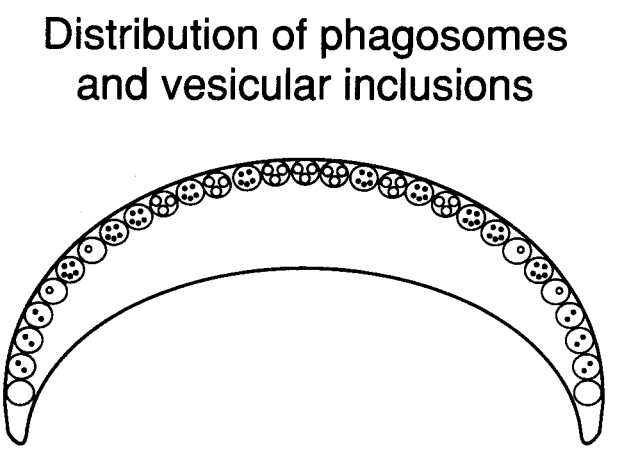

FIGURE 12. Schematic semiquantitative drawing of the distribution of phagosomes (and phagolysosomes) and vesicular inclusions in the deep-sea fish retina. In the extreme periphery of the retina RPE cells contain no phagosomes and no vesicular inclusions. In the mid-periphery RPE cells contain few phagosomes and few vesicular inclusions. In the central retina RPE cells contain many phagosomes and many and large vesicular inclusions. ⊙ represents few, ⊛ represents many phagosomes and phagolysosomes, ⊙ represents few, ⊕ represents many large vesicular inclusions.

This suggests that young rods synthesize more disc material which might give them an increased sensitivity for photon absorption. This conclusion supports the concept of Shapley and Gordon (1980) who found that in the multibank retina of the conger eel only vitread rods produced a normal ERG response.

Phagosomes

We detected phagosomes of different stages in the RPE cells of all species investigated. Although phagosomes containing clearly visible undigested disc membranes were more frequent, we also observed phagolysosomes. The presence of phagolysosomes indicates that the ingestion of ROSs was not mainly caused by unphysiological conditions during the catch of the fish. The different number of phagosomes/mm in the central and in the peripheral retina (Table 2, Fig. 12, schematic drawing) provides evidence that shedding occurred *in vivo* because shedding induced during the towing of the net should lead to a similar degree of phagocytosis in all areas of the retina. In addition to conventional phagosomes we observed electron-lucent vesicular inclusions in the RPE cells which were more prominent in the central retina and in larger animals. Similar inclusions are not found in the normal RPE of vertebrates. However, they were observed in retinae with degenerative diseases (Watson *et al.*, 1993). Defects of lysosomal enzymes have also been implicated in the occurrence of vesicular inclusions in the RPE (Aguirre *et al.*, 1995). These inclusions may be related to a defective or reduced phagocytotic potential of the RPE cells. The occurrence of macrophages in the OS layer and the subretinal space is unusual. They are present in ocular diseases and were observed after photoreceptor damage by light exposure (Hoppeler *et al.*, 1988). It is conceivable that the high illumination levels during the catch and preparation caused an invasion of macrophages in the outer retina of our deep-sea fish.

Rod outer segment lengths

Rod outer segments were longer in the peripheral than in the central part of the retina (Figs 9 and 13, schematic drawing). Although ROSs, on the average, were shorter in large than in small specimens the distribution of ROS lengths appears to be similar in small and in large animals. Remarkably, in the periphery, the predominance of long ROSs coincides with the occurrence of RPE cells containing no or only few phagosomes.

The size-related decrease of ROS lengths in multibank retinae (*N. armatus*, *C. guentheri*) was similar to that reported for other vertebrates (Fox & Rubinstein, 1989). The higher degree of size-related decrease in ROS lengths in the single or double bank retina (*C. macroptera*, *S. kaupi*) may be due to a higher shedding activity. This can be assumed because in these species RPE cells are located closer to the ROS tips. Shedding appears to take place at slightly lower rates in large fish (Fig. 7). By contrast, the low number of PCVs in the

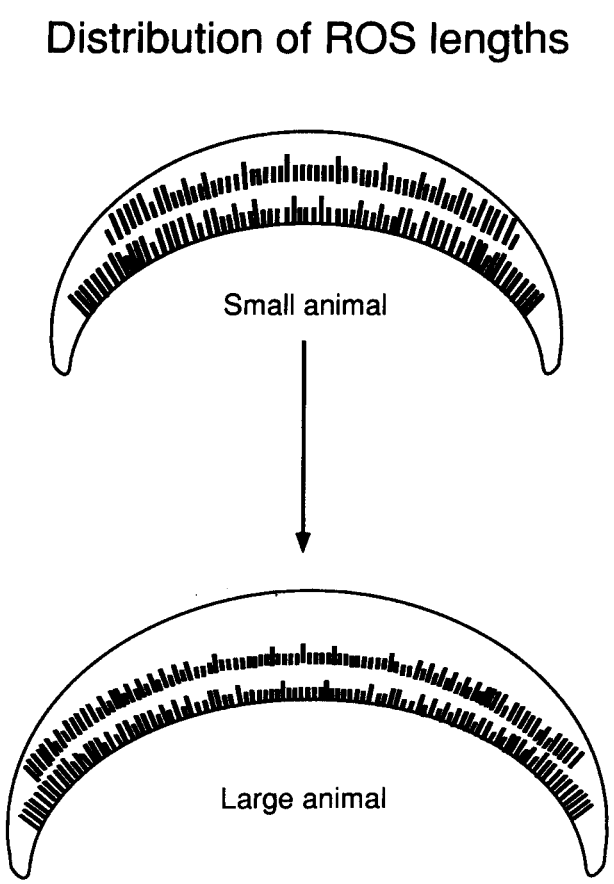

FIGURE 13. Schematic semiquantitative drawing of the distribution of ROS lengths in small and large individuals. ROSs are longer in small than in larger animals. Long ROSs predominate in the peripheral retina of all retinae.

sclerad RISs of multibank retinae, and the generally low number of PCVs in the RISs of all larger retinae suggests that the synthesis of disc material is markedly reduced in larger (older) animals. The imbalance of disc formation and shedding may account for the observed decrease in ROS lengths.

In our preparations of dissociated retinae no significant difference was observed in the length of vitread vs sclerad ROSs. However, from the number of PCVs per RIS we conclude that vitread RISs synthesize more disc material than sclerad ones. This would indicate that vitread ROS tips are similarly shed and an increase in length is prevented. However, since RPE processes seem to be unable to reach the tips of the most vitread ROSs the exact mechanism of shedding, phagocytosis, and degradation is unclear. We can only speculate how shedding of the tips of vitread ROSs might be achieved. ROSs may be able to approach the RPE cells by active elongation of their myoids in a process reminiscent of retinomotor movements in other fish retinae. Alternatively, macrophages are possible candidates for the digestion of discs and removal of ROS tips. These cells should be able to recognize the respective ROSs and be present predominatly in the more vitread part of the ROS layer. A corresponding higher incidence of macrophages in this part of the ROS layer was not observed in our material. However, in vertebrate retinae, a low portion of the proteases in the RPE cells is secreted into the subretinal space (Adler, 1989). In the retinae of deep-sea fish with possibly low rates of shedding, this process may be sufficient to digest the discs partially. Migrating retinal macrophages may then remove and degrade the debris completely.

In conclusion, our findings suggest that there is no uniform mechanism of OS renewal in the retinae of deep-sea fish. In all species, synthesis of OS discs (as reflected by the number of PCVs) is most active in the retinal periphery. At the same time, the density of phagosomes is lowest in this area and ROSs are longer in this region than in the central fundus. This is especially true for species with single or double bank retinae. In species with multibank retinae, the innermost layer of rods contains more PCVs than the outermost layer. Since low levels of light in the abyssal environment would render repair mechanisms unlikely, it is tempting to suggest that the increased synthetic activity in the vitread bank of rods results in a higher capacity for photon catch and eliciting a visual response. This concept is consistent with the ERG measurements of Shapley and Gordon (1980). At the same time, our findings would confirm earlier suggestions that rods in the most sclerad banks are less functional. In this view, in multibank retinae "used" rods would be "displaced" away from the incoming light and stored near Bruch's membrane instead of being totally removed by the RPE (Denton & Locket, 1989).

REFERENCES

Adler, A. J. (1989). Selective presence of acid hydrolases in the interphotoreceptor matrix. *Experimental Eye Research, 49*, 1067–1077.

Aguirre, G., Ray, L., Pearce-Kelling, S., Stramm, L. & Haskins, M. (1995). Lysosomal mannosidase is essential for retinal pigment epithelial (RPE) degradative function. *Investigative Opthalmology and Visual Science, 36*, 816.

Bosch, E., Horwitz, J. & Bok, D. (1993). Phagocytosis of outer segments by retinal pigment epithelium: Phagosome–lysosome interaction. *Journal of Histochemistry and Cytochemistry, 41*, 253–263.

Crescitelli, F., McFall-Ngai, M. & Horwitz, J. (1985). The visual pigment sensitivity hypothesis: Further evidence from fishes of varying habitats. *Journal of Comparative Physiology A, 157*, 323–333.

Denton, E. & Locket, N. (1989). Possible wavelength discrimination by multibank retinae in deep-sea fishes. *Journal of the Marine Biological Association of the United Kingdom, 69*, 409–435.

Eckmiller, M. (1989). Outer segment growth and periciliary vesicle turnover in developing photoreceptors of *Xenopus laevis*. *Cell and Tissue Research, 255*, 283–292.

Fox, D. A. & Rubinstein, S. D. (1989). Age-related changes in retinal sensitivity, rhodopsin content and rod outer segment length in hooded rats following low-level lead exposure. *Experimental Eye Research, 48*, 237–249.

Fröhlich, E., Negishi, K. and Wagner, H.-J. (1995a). Mechanisms of rod proliferation in deep-sea fish retinae. *Vision Research, 35*, 1799–1811.

Fröhlich, E., Negishi, K. and Wagner, H.-J. (1995b). The occurrence of dopaminergic interplexiform cells correlates with the presence of cones in the retinae of fish. *Visual Neuroscience, 12*, 359–369.

Hoppeler, T., Hendrickson, P., Dietrich, C. & Remé, C. (1988).

Morphology and time-course of defused photochemical lesions in the rabbit retina. *Current Eye Research, 7*, 849–860.

Locket, N. (1980). Variation of the architecture with size in the multiple-bank retina of a deep-sea teleost, *Chauliodus sloani. Proceedings of the Royal Society London B, 208*, 223–242.

Merrett, N. R. & Marshall, N. B. (1981). Observations on the ecology of deep-sea bottom-living fishes collected off northwest Africa (08°–27°N). *Progress in Oceanography, 9*, 185–244.

Powers, M. K. & Raymond, P. A. (1990). Development of the visual system. In Douglas, R. H. & Djamgoz, M. B. A. (Eds), *The visual system of fish* (pp. 419–442). London: Chapman & Hall.

Richardson, K., Jarett, L. & Finke, E. (1960). Embedding in epoxy resins for ultrathin sectioning in electron microscopy. *Stain Technology, 35*, 313–323.

Roof, D. J. (1986). Turnover of vertebrate photoreceptor membranes. In Stieve, H. (Ed.), *The molecular mechanism of photoreception* (pp. 287–302). Berlin: Springer.

Shapley, R. & Gordon, J. (1980). The visual sensitivity of the conger eel. *Proceedings of the Royal Society London B, 209*, 317–330.

Watson, P., Wigstad, A., Riies, R. C., Narfstrom, K., Bredfort, P. G. C. & Nilsson, S. E. G. (1993). Retinal degeneration in the Briard dog. In Hollyfield, J. G., Anderson, R. E. & LaVail, M. M. (Eds.), *Retinal degeneration* (pp. 281–290). New York: Plenum Press..

Young, R. (1971). The renewal of rod and cone outer segments in the rhesus monkey. *Journal of Cell Biology, 49*, 303–318.

Acknowledgements—We are most grateful to the British NERC for inviting one of us (H.-J. W.) to participate in cruises 94 and 122 of RRS Challenger. Furthermore, we are indebted to the Master and the Crew of the RRS Challenger and to Drs I. G. Priede and J. C. Partridge for organizing the cruises as PSOs. Thanks also to the other members of the Challenger I-Team (Drs R. H. Douglas, J. C. Partridge, S. P. Collin, T. Onic and A. Gordon) for many stimulating discussions. We thank Frau B. Klaas and B. Aichele for careful help with the histology and M. Mauz for photographic work.